

Numerical Modelling of the Primary Source in a Hemi-Anechoic Room

*Original*

Numerical Modelling of the Primary Source in a Hemi-Anechoic Room / Arina, Renzo; Volkel, Katharina. - CD-ROM. - Proceedings of INTER-NOISE 2016:(2016). (Intervento presentato al convegno INTER-NOISE 2016 tenutosi a Hamburg, Germany nel 21-24 August).

*Availability:*

This version is available at: 11583/2648932 since: 2016-09-14T13:48:00Z

*Publisher:*

*Published*

DOI:

*Terms of use:*

openAccess

This article is made available under terms and conditions as specified in the corresponding bibliographic description in the repository

*Publisher copyright*

(Article begins on next page)

## Numerical modeling of the primary source in a hemi-anechoic room

R. Arina<sup>1</sup>, K. Völkel<sup>2</sup>

<sup>1</sup>Politecnico di Torino, Torino, Italy

<sup>2</sup>Physikalisch Technische Bundesanstalt, Braunschweig, Germany

### ABSTRACT

An effective use of the primary source requires a deep knowledge and understanding of the governing phenomena that influence its sound power output. The paper reports on a numerical model for describing the acoustic behavior of the primary source in an hemi-anechoic room. The wave equation is discretized in the frequency space with a high-order Finite Element method. Fully reflecting boundary conditions are imposed along the room floor, while suitable partially-reflecting boundary conditions, using absorbing layers, are specified on the anechoic walls to mimic real conditions. In the free-field computation the lining is considered as perfectly absorbing, and in real case reflective properties are considered. The major primary source properties, such as sound power and directivity index are calculated for low frequencies. Challenge is here to separate the effects of the wall room reflections from the source properties.

Keywords: Sound power, Free Field, Directivity

### INTRODUCTION

The sound emission of a source is most objectively described by its sound power output. Consequently there are several standardized procedures for the determination of the sound power of a source. Until now all of these measurements suffer from the lack of primary standard for the realization of the unit Watt in airborne sound. Such a primary sound source was developed as part of the European Metrology Research Programme SIB 56. This source is based on a vibrating baffled piston [2].

Measurements with this device are carried out in PTB's hemi-anechoic room which provides an approximation of a free sound field. Two distinct measurement procedures are applied to obtain the sound power of the primary standard: the first method employs a laser-scanning vibrometer that scans the surface of the primary source and records data on vibration velocity and phase. For the second method sound pressure levels are measured on a hemispherical surface around the source and sound powers are calculated according to ISO 3745.

The frequency range measured with the primary source extends from 20 Hz to 20 kHz. It is known that the sound field assumption is of utmost importance in the determination of correct sound power levels when these are calculated from sound pressure measurements [3]. Thus, the main limiting factor in the comparability of the sound power levels obtained by the two described methods is the ability of PTB's hemi-anechoic room to provide a good approximation of a free field. This is especially relevant for low frequencies. For this reason a numerical study was conducted that contrasted the sound power measured for a monopole in either PTB's hemi-anechoic room or in a room of the same geometry but providing a perfect free field. Three single frequencies were chosen for a first test and are reported here. They are 50 Hz, 100 Hz and 150 Hz.

### HEMI-ANECHOIC ROOM AT PTB

The hemi-anechoic room at PTB has a pentagonal sound reflecting base plate (Fig. 1). Free field conditions are achieved through the use of sound absorbing wedges of length 0.80 m. These are installed on all room walls as well as the ceiling. With wedges installed, the room height is 4.65 m and the longest side lengths

<sup>1</sup>email: [renzo.arina@polito.it](mailto:renzo.arina@polito.it)

<sup>2</sup>email: [katharina.voelkel@ptb.de](mailto:katharina.voelkel@ptb.de)

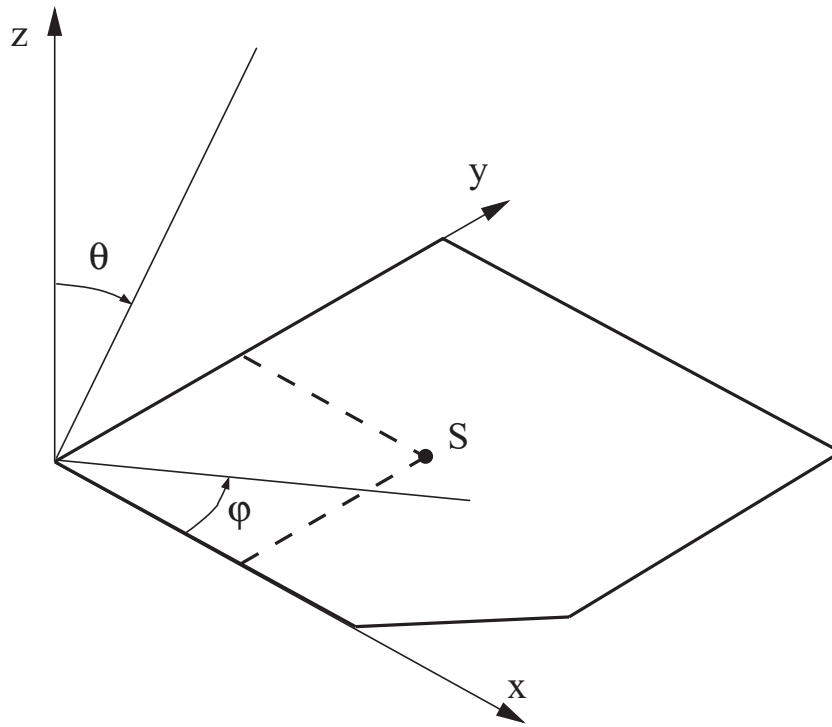


Figure 1: Reference frame for directivity indexes.

are 6.5 m and 6.25 m, respectively. The volume of the room is 184.1 m<sup>3</sup> with wedges and 337.4 m<sup>3</sup> without wedges.

To assess the quality of the free field achieved in this room, the absorption coefficients of two sets of wedges consisting of two wedges each were measured in a Kundt's tube. The absorption coefficients averaged over six measurements were then supplied as boundary condition for the numerical simulation of PTB's hemi-anechoic room (Fig. 2).

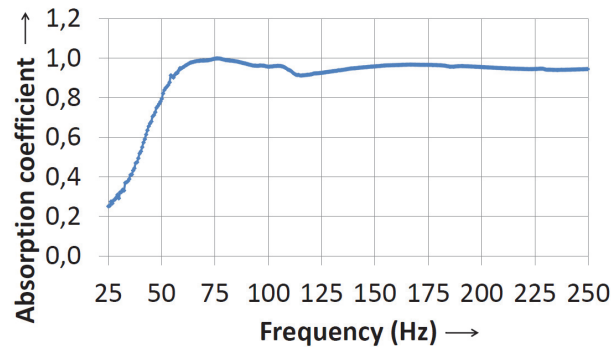


Figure 2: Absorption coefficients of the wedges in PTB's hemi-anechoic room for different frequencies.

## NUMERICAL SIMULATIONS

Propagation of acoustic waves in still air is governed by the linearized Euler equations which reduce into a scalar wave equation for the pressure (or density) fluctuations. For time-harmonic problems the wave equation reduces to the Helmholtz equation.

The main purpose of the present work, to compare the acoustic behavior of a monopole in a perfect and a real hemi-anechoic chambers, is to model the acoustic propagation in the confined chamber with appropriate boundary conditions able to mimic as close as possible the real absorbing and reflecting characteristics of the vertical walls and the ceiling.

In the case of perfectly non-reflecting walls, a widely used technique to prevent numerical reflections is the so-called Perfectly Matched Layer (PML) method [4]. It consists into the construction of a layer exterior to

the domain of interest damping all the waves that enter from the interior domain. This layer is represented by a modified Helmholtz equation which is not necessarily physically realizable. The uniqueness of the PML method is that the dissipation properties are essentially independent of the angle of incidence and also of the frequency of the incoming wave. The method consists in introducing a fictitious complex stretching of the spatial variables  $(x, y, z)$ , with the substitution  $\partial/\partial x \rightarrow s_x(x)\partial/\partial x$ , where

$$s_x = 1 + \frac{\sigma_x(x)}{ik},$$

with  $k$  the wave number. The modified Helmholtz equation reads

$$\frac{\partial}{\partial x} \left( \frac{s_y s_z}{s_x} \frac{\partial p}{\partial x} \right) + \frac{\partial}{\partial y} \left( \frac{s_x s_z}{s_y} \frac{\partial p}{\partial y} \right) + \frac{\partial}{\partial z} \left( \frac{s_x s_y}{s_z} \frac{\partial p}{\partial z} \right) + s_x s_y s_z k^2 p = 0. \quad (1)$$

Outside the PML regions,  $\sigma_x = \sigma_y = \sigma_z = 0$  and the modified equation (1) reduces to the Helmholtz equation. No reflections at the interface between the interior domain and the PML occur if  $\sigma_x(x) > 0$  and varies at least linearly inside the sponge layer, and the PML width is large enough to have a complete damping.

To mimic partially reflecting walls, it is proposed to employ a *partially absorbing* PML boundary condition, by an appropriate choice of a constant value of  $\sigma_x$ ,  $\sigma_y$  and  $\sigma_z$ . The selection of the correct value of the  $\sigma$  functions is based on experimental data of the absorption coefficient measured in a Kundt's tube. The calibration procedure is obtained solving the acoustic problem in the impedance tube replacing the absorbing end wall with a PML boundary condition. Evaluating the sound pressure at two points,  $x_1$  and  $x_2$ , inside the tube, in the case of harmonic plane waves the transfer function  $H_{12} = \hat{p}_2/\hat{p}_1$  is related to the reflection coefficient  $R$  as, with  $\Delta = x_2 - x_1$ ,

$$R = \frac{H_{12} - e^{ik\Delta}}{e^{-ik\Delta} - H_{12}} e^{-2ikx_1}.$$

The absorption coefficient is obtained as

$$\alpha = \frac{(p_i)_{rms} - (p_r)_{rms}}{(p_i)_{rms}} = 1 - |R|^2.$$

In Table (1) are reported the values of the function  $\sigma$  for different frequencies and the computed absorption coefficients  $\alpha$ . The numerical values of the absorption coefficient are close to the measured values in the case of the PTB hemi-anechoic chamber reported in Figure (2).

The numerical solution of the acoustic pressure field generated by a monopole placed near the floor of the PTB hemi-anechoic chamber is obtained solving the Helmholtz equation with a FEM discretization and imposing fully reflecting boundary conditions on the floor and PML conditions on the vertical walls and the ceiling. The FEM system is solved using the FreeFem++ software [5].

## DATA ANALYSIS

Data analysis focused on a hemisphere with radius 1.5 m centered on the floor with x- and y-coordinates corresponding to those of the monopole source. Frequencies considered were 50 Hz, 100 Hz and 150 Hz. For each frequency, directivity indexes were calculated both for the real hemi-anechoic room as well as the ideal free field as

$$DI = 10 \log_{10} \left( \frac{p_i^2}{p_{ref}^2} \right) \quad dB.$$

The reference sound pressure used was that recorded along the z-axis. The directivity indexes corresponded to arcs along the hemisphere with  $\varphi = 0^\circ$ ,  $\varphi = 45^\circ$  or  $\varphi = 90^\circ$  (Fig. 1). Secondly, sound power levels ( $L_W$ ) for both the ideal as well as the real room were calculated for each frequency by averaging the sound pressure levels on a mean square basis ( $\overline{L_p}$ ) and taking into account the hemispherical measurement surface ( $S$ ) referenced to the value  $S_0 = 1 \text{ m}^2$ , as follows

$$L_W = \overline{L_p} + 10 \log_{10} \left( \frac{S}{S_0} \right) \quad dB.$$

Table 1: PML coefficient and numerical absorption coefficient in function of the frequency

$f \text{ Hz}$	$\sigma$	$\alpha$
20	0.150	0.180247
30	0.350	0.371084
40	0.600	0.548428
50	1.100	0.767195
60	1.700	0.89485
70	2.400	0.958402
80	3.100	0.983531
90	3.400	0.988932
100	3.400	0.988942
125	4.500	0.997413
150	5.000	0.998685
175	7.000	0.999908
200	8.000	0.999972
225	8.000	0.999973
250	8.000	0.999975
275	8.000	0.999971
300	5.000	0.998699

## RESULTS

Results show that at 50  $\text{Hz}$  and 100  $\text{Hz}$  there is a significant difference in sound power levels obtained for the real and ideal room. This difference becomes negligible at 150  $\text{Hz}$  (Tab. 2). This shows that the hemi-anechoic room at PTB does not provide a good free sound field up to a frequency of 100  $\text{Hz}$ . At a frequency of 150  $\text{Hz}$  though, the sound field in the measurement room at PTB is a good approximation of a free field.

Table 2: Comparison of sound power levels for ideal and real room

Frequency ( $\text{Hz}$ )	$L_{W,\text{ideal}} \text{ (dB)}$	$L_{W,\text{real}} \text{ (dB)}$	$\Delta L_{W,\text{real-ideal}} \text{ (dB)}$
50	80.0	80.9	0.83
100	92.3	92.9	0.61
150	96.1	96.2	0.08

The sound power results are confirmed by plots of the directivity of sound emission for different values of the azimuthal angle,  $\varphi$ . At 50  $\text{Hz}$  (Fig. 3) and 100  $\text{Hz}$  (Fig. 4) an influence of the cut off corner in the geometry of PTB's measurement room is visible for both the ideal as well as the real sound fields. This is due to the sharp slope change at that corner which introduces spurious reflections in the numerical model. However, comparing the directivity plots of real and ideal test rooms, it is evident that there are reflections from the walls of PTB's hemi-anechoic room which obliterate the uniform sound emission of the tested monopole to some extent.

These effects vanish at 150  $\text{Hz}$  (Fig. 3). The directivities for the monopole in the real and ideal test room show no significant difference for that frequency. There is also no effect of the non-perfect rectangular geometry of the test rooms anymore. This confirms the results obtained in the comparison of sound power levels: PTB's hemi-anechoic room provides a good approximation of a free field at 150  $\text{Hz}$ .

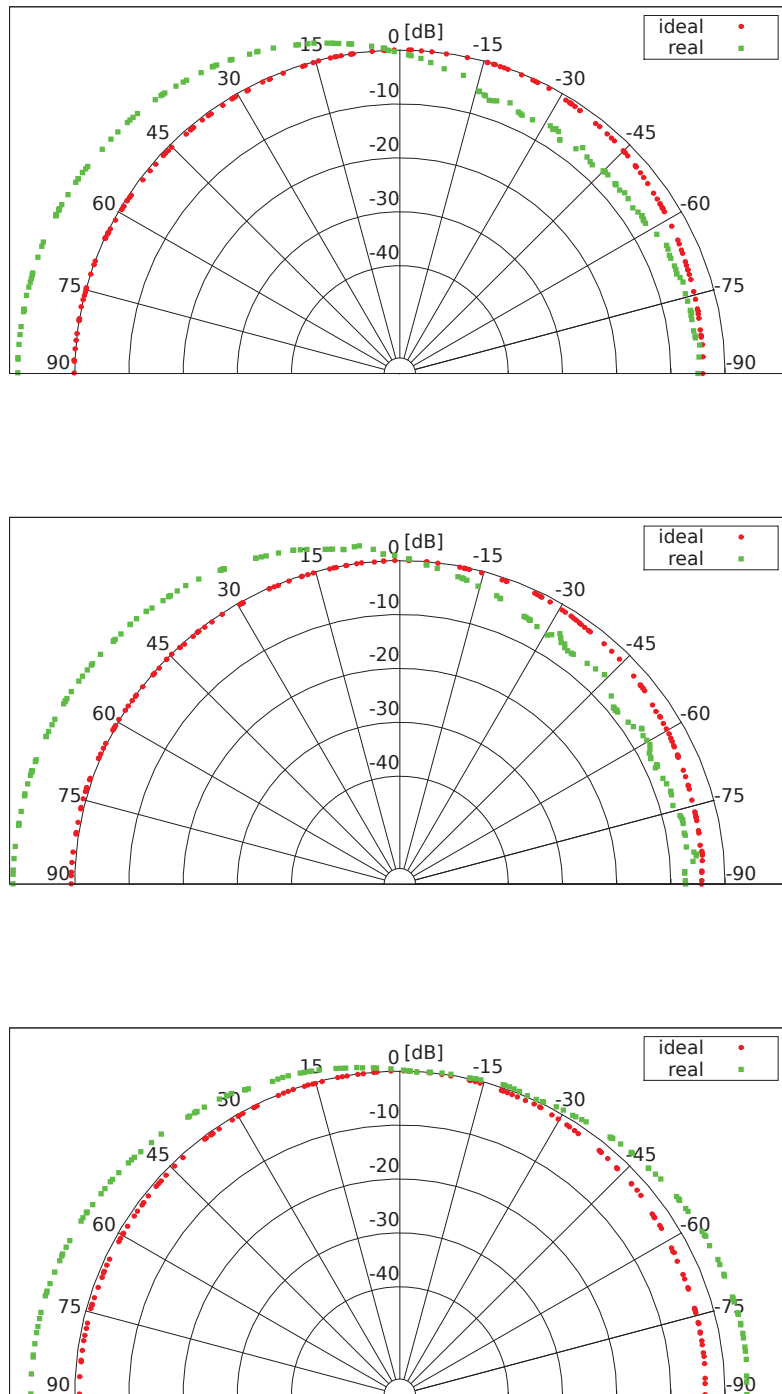


Figure 3: Directivity indexes at  $f = 50 \text{ Hz}$  for  $\varphi = 0^\circ$ ,  $\varphi = 45^\circ$  and  $\varphi = 90^\circ$  from top to bottom.

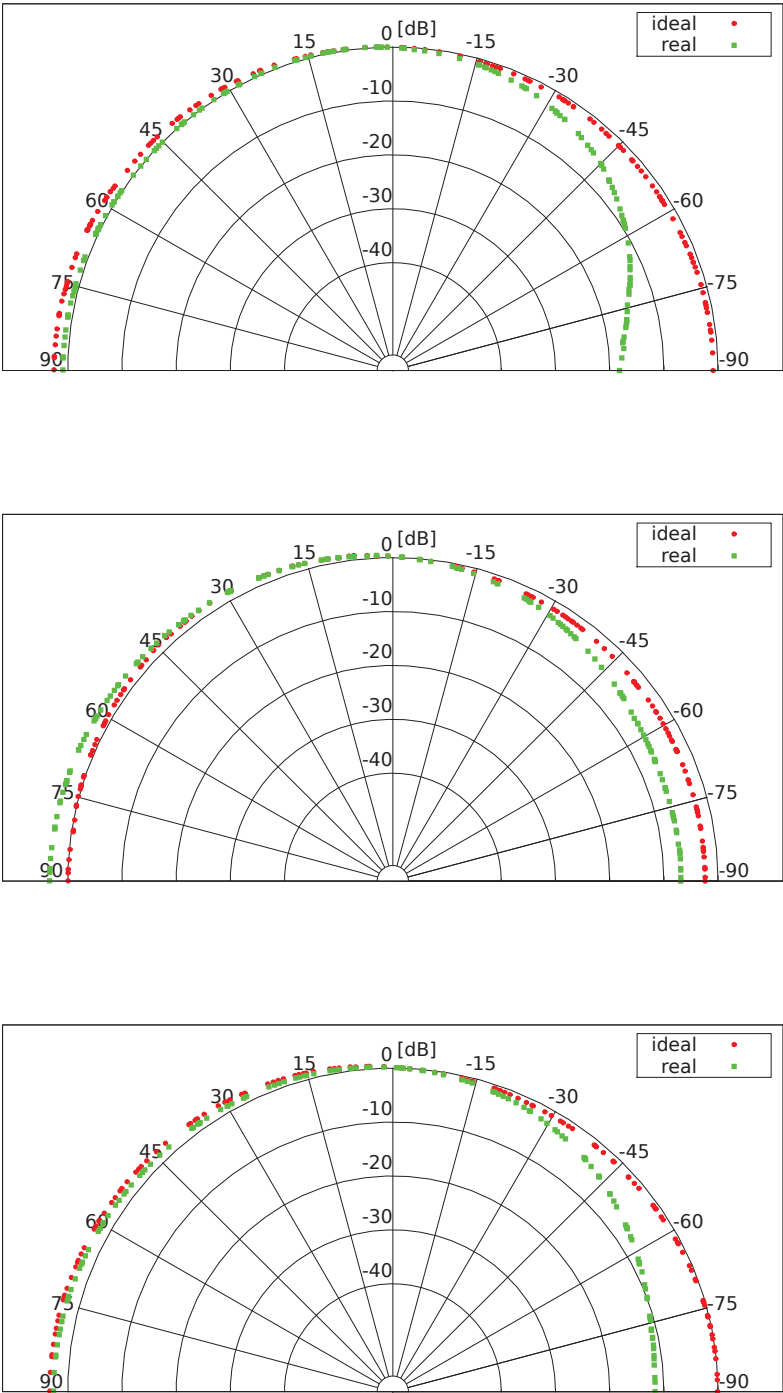


Figure 4: Directivity indexes at  $f = 100 \text{ Hz}$  for  $\varphi = 0^\circ$ ,  $\varphi = 45^\circ$  and  $\varphi = 90^\circ$  from top to bottom.

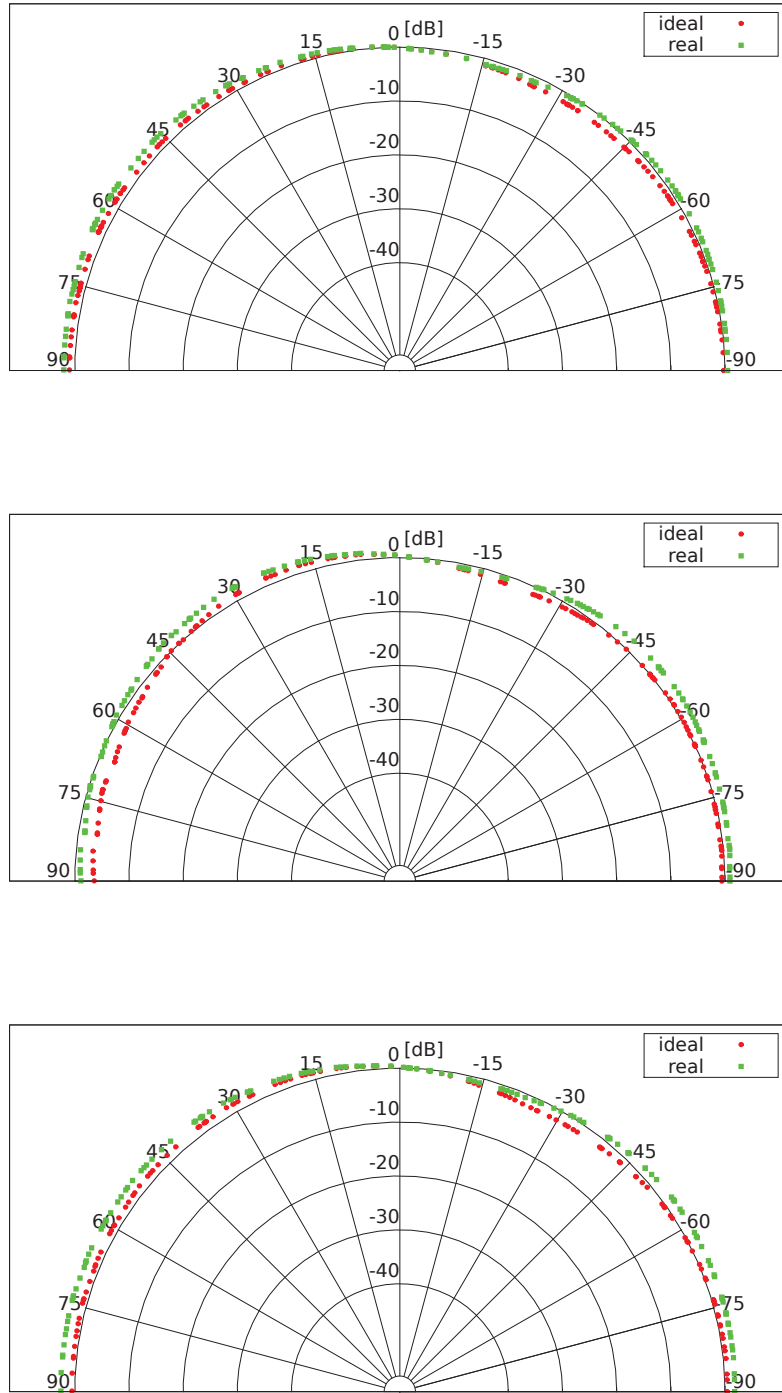


Figure 5: Directivity indexes at  $f = 150$  Hz for  $\varphi = 0^\circ$ ,  $\varphi = 45^\circ$  and  $\varphi = 90^\circ$  from top to bottom.



This paper presented first results on a comparison of sound power levels and directivities for a monopole source in a perfect free field vs. a real measurement room. Investigating three frequencies (50 *Hz*, 100 *Hz* and 150 *Hz*) it was shown that the real measurement room at PTB does not provide a good free field at or below 100 *Hz*. This result needs to be considered when comparing sound power levels obtained for the primary sound source using a laser-scanning vibrometer vs. pressure measurements. A more detailed study is needed to define the lower frequency limit for PTB's hemi-anechoic room as well as to investigate and quantify whether effects are more or less pronounced using FFT or one-third octave band analysis.

## **ACKNOWLEDGMENT**

The work presented in this paper is part of the European Metrology Research Programme (EMRP) joint research project SIB 56 "SoundPwr". The EMRP is jointly funded by the EMRP participating countries within EURAMET and the European Union.

## **REFERENCES**

- [1] ISO 3745:2012 Acoustics – Determination of sound power levels and sound energy levels of noise sources using sound pressure – Precision methods for anechoic rooms and hemi-anechoic room
- [2] Wittstock, V., Schmelzer, M., Bethke, C.: Establishing traceability for the quantity sound power. *Proceedings of Internoise*, 2013.
- [3] Wittstock, V.: A new approach in sound power metrology. *OIML Bulletin*, 55(2):9-13, 2014.
- [4] Abarbanel S. and Gottlieb D., A mathematical analysis of the PML method, *J. Comput. Physics*, 134:357-363, 1997.
- [5] Hecht F., New developments in FreeFem++, *J. Numer. Meth.*, 20(3-4):251-265, 2012.